AGU PUBLICATIONS

Water Resources Research

RESEARCH ARTICLE
10.1002/2016WR018906

A 277 year cool season dam inflow reconstruction for Tasmania, southeastern Australia

K. J. Allen [1], S. C. Nichols[1], R. Evans[1,2], S. Allie [3], G. Carson [3], F. Ling[4], E.R. Cook [5], G. Lee[6], and P. J. Baker [1]

[1]School of Ecosystem and Forest Sciences, University of Melbourne, Richmond, Victoria, Australia, [2]Silviscan Pty Ltd, Doncaster East, Victoria, Australia, [3]Hydro Tasmania, Hobart, Australia, [4]Entura Consulting, Hydro Tasmania, Cambridge, Australia, [5]Lamont-Doherty Earth Observatory, Palisades, New York, USA, [6]Antarctic Climate and Ecosystems Cooperative Research Centre, University of Tasmania, Hobart, Australia

Key Points:
- First cool season hydroclimatic reconstruction for southeastern Australia shows drier conditions more common in most recent 150 years
- Recent July–August hydroclimate within natural variability of the past 277 years
- Latewood cell wall thickness chronology most important predictor in model

Supporting Information:
- Supporting Information S1

Correspondence to:
K. J. Allen,
Kathryn.Allen@unimelb.edu.au

Citation:
Allen, K. J., S. C. Nichols, R. Evans, S. Allie, G. Carson, F. Ling, E. R. Cook, G. Lee, and P. J. Baker (2017), A 277 year cool season dam inflow reconstruction for Tasmania, southeastern Australia, *Water Resour. Res.*, *53*, 400–414, doi:10.1002/2016WR018906.

Received 8 MAR 2016
Accepted 29 NOV 2016
Accepted article online 17 DEC 2016
Published online 17 JAN 2017

Abstract Seasonal variability is a significant source of uncertainty in projected changes to precipitation across southeastern Australia (SEA). While existing instrumental records provide seasonal data for recent decades, most proxy records (e.g., tree rings, corals, speleothems) offer only annual reconstructions of hydroclimate. We present the first cool-season (July–August) reconstruction of dam inflow (Lake Burbury) for western Tasmania in SEA based on tree-ring width (*Athrotaxis selaginoides*) and mean latewood cell wall thickness (*Phyllocladus aspleniifolius*) chronologies. The reconstruction, produced using principal component regression, verifies back to 1731 and is moderately skillful, explaining around 23% of the variance. According to the reconstruction, relatively low inflow periods occurred around 1860, the early 1900s and 1970, while relatively high inflows occurred in the 1770s and 1810s. Highest reconstructed inflows occurred in 1816, and lowest in 1909. Comparison with available documentary and instrumental records indicates that the reconstruction better captures high rather than low flow events. There is virtually no correlation between our reconstruction and another for December–January inflow for the same catchment, a result consistent with the relationship between seasonal instrumental data. This suggests that conditions in one season have not generally reflected conditions in the other season over the instrumental record, or for the past 277 years. This illustrates the value of obtaining reconstructions of regional hydroclimatic variability for multiple individual seasons in regions where dry and wet seasons are not strongly defined. The results also indicate that the hydroclimate of the southeastern Australian region cannot be adequately represented by a single regional reconstruction.

1. Introduction

Australia's climate is one of the most variable in the world, and both drought and flooding rains have long captivated poets (e.g., McKellar's "I Love A Sunburnt Country", Hartigan's "Said Hanrahan") and climatologists [e.g., *Allen*, 1895; *Nichols*, 2010; *Larsen and Nichols*, 2009; *Verdon-Kidd and Kiem*, 2009; *Power and Callaghan*, 2016, amongst many others]. However, instrumental records that typically span less than 100 years do not capture the full range of natural variability inherent in the Australian hydroclimate, particularly at decadal to centennial time scales. As climate changes, the need to better understand long-term hydroclimatic variability in Australia, including the occurrence of extreme events like drought and flood, has become increasingly pressing [*Kiem et al.*, 2016]. To this end, a number of annually resolved Australian palaeohydrological records have been published over the past two decades [e.g., *Isdale et al.*, 1998; *Cullen and Grierson*, 2009; *McGowan et al.*, 2009; *Lough*, 2011; *Gallant and Gergis*, 2011; *Gergis et al.*, 2011; *Vance et al.*, 2014; *Allen et al.*, 2015a; *Ho et al.*, 2015; *Tozer et al.*, 2016]. Most recently, *Palmer et al.* [2015] have captured spatial and temporal variability in the summer hydroclimate over much of eastern Australia for the past 500 years. However, almost all previous reconstructions for southeastern Australia [i.e., *McGowan et al.*, 2009; *Gallant and Gergis*, 2011; *Gergis et al.*, 2011; *Vance et al.*, 2014; *Ho et al.*, 2015; *Tozer et al.*, 2016] have reconstructed hydroclimatic conditions for annual time slices. For regions where precipitation is not primarily limited to a specific season (e.g., "the wet season" in Australia's far north), but is instead distributed across the year, annual records will obscure important seasonal variation in precipitation variability [see

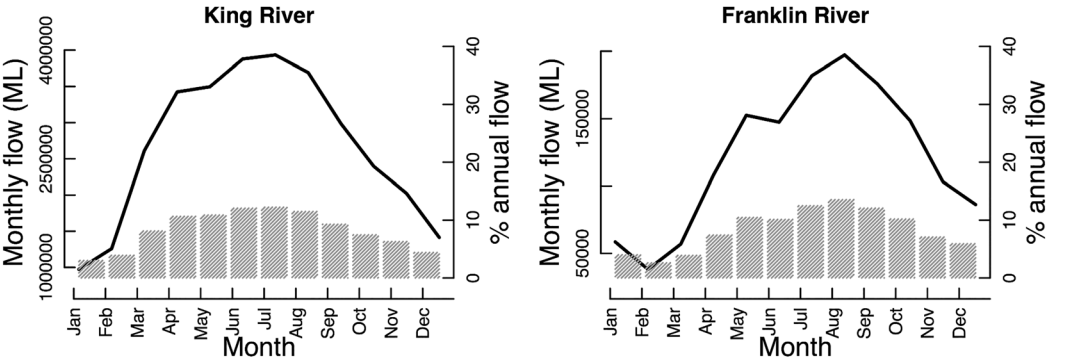

Figure 1. Average monthly streamflow for King and Franklin Rivers, central western Tasmania. Location of King River gage shown in Figure 2. Franklin River gage is ~25km ESE of King River gage. Line plot shows measured flow (ML) and bars indicate percentage of total annual flow for each month's flow. Flow is lowest from January–March, and highest from June–September.

Drosdowsky, 1993; *Murphy and Timbal*, 2008; *Risbey et al*., 2009; *Cai et al*., 2011;*Timbal and Drosdowsky*, 2013 amongst others]. In far southeastern Australia (SEA), more precipitation falls in the cooler months but substantial amounts can still fall during warm months. The average seasonal percentages of total annual precipitation for major west Tasmanian catchments are: 17.8% in summer; 24.4% in autumn, 31.5% in winter, and 26.3% in spring. These patterns are matched by seasonal streamflows in the central west where the study area (see below) is located (Figures 1 and 2).

Seasonally defined variability is particularly relevant in regions such as SEA because the dominant drivers of precipitation vary geographically and seasonally [*Pook et al*., 2006; *Risbey et al*., 2009; *Allen et al*., 2015b]. The El Niño Southern Oscillation (ENSO), the Interdecadal Pacific Oscillation (IPO), the Southern Annular mode (SAM), the Indian Ocean Dipole (IOD), and atmospheric blocking dipole systems are the dominant precipitation drivers over the general SEA region. Complex interactions among these drivers lead to substantial interannual and interdecadal variability in precipitation.

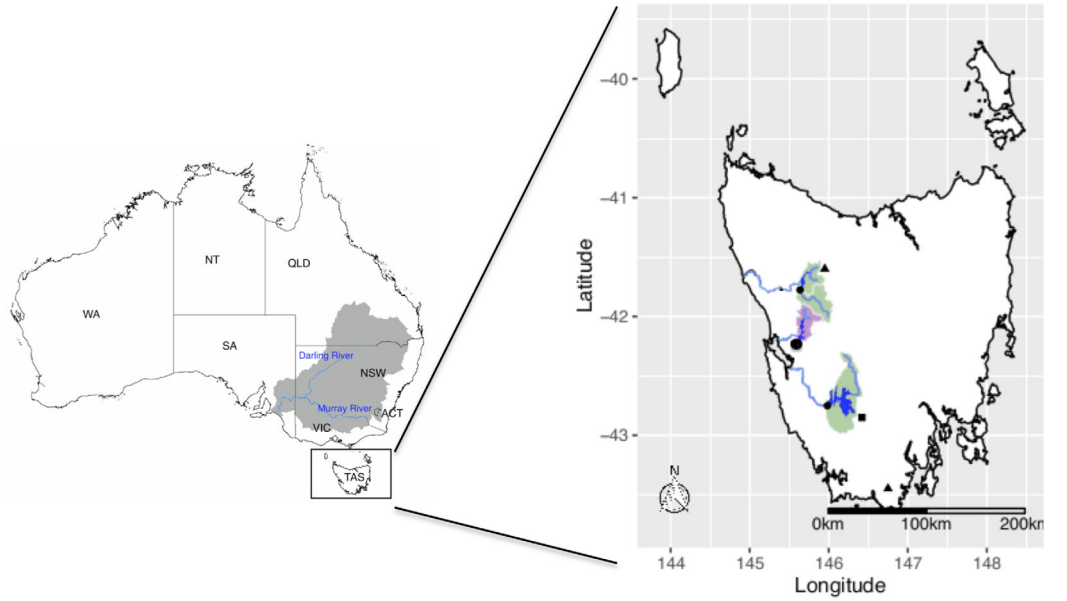

Figure 2. (right) Site map and (left) relative location in southeastern Australia. Murray Darling Basin (MDB) and states and territories also shown on the map of Australia. Major west Tasmanian catchments used to generate hydroelectricity and tree ring sites shown on map of Tasmania. Most southern catchment is Gordon, next is Burbury (pink) for which inflows have been reconstructed, then Murchison and Mackintosh make up the two parts of the most northern catchment. Tree-ring width sites (solid triangle), the TNE latewood cell wall thickness chronology (sloid square), and dam inflow measurement sites (solid circle) are also shown. Lake Burbury inflow measurement site is larger circle. Location of main rivers flowing through catchments shown; the King River flows into, and out of the Lake Burbury catchment. Data used in map of Tasmania are courtesy of Hydro Tasmania.

An atmospheric blocking dipole system is composed of a quasi-stationary anticyclone to the south of the subtropical ridge (STR) [*Pook et al*., 2013] and a cutoff cyclone to the north. The quasi-stationary anticyclone represses rainfall over part of southern Australia (e.g., Tasmania's west coast) while the cutoff cyclone can be responsible for very heavy falls along the eastern seaboard [*Risbey et al*., 2009; *Pook et al*., 2013]. These systems have greatest influence on west Tasmanian rainfall in the autumn-spring months [*Risbey et al*., 2009]. SAM's main impact on west Tasmanian precipitation occurs mainly from winter to summer [*Risbey et al*., 2009], and it also has an important influence on precipitation in more northern parts of SEA in the spring and summer months. ENSO's widespread impact on Australian precipitation is well known [*McBride and Nicholls*, 1983; *Allan*, 1988]; however, its strongest impacts are generally on eastern Australia in the spring months. However, ENSO is not independent of other ocean-atmosphere processes such as the IOD [*Meyers et al*. 2007], IPO, and SAM [*Pezza et al*., 2012]. After removing the influence of the IOD, ENSO has its greatest influence on precipitation across northeastern Australia and eastern Tasmania in the cooler months of June–October [*Risbey et al*., 2009]. The low-frequency IPO modulates the impact of ENSO on SEA rainfall and its positive phase is associated with anomalously dry conditions while its negative phase is associated with higher precipitation over SEA [*Power et al*., 1999]. The IOD's strongest relationship with precipitation, independent of ENSO, occurs for a band of Australia extending from the northwest to the southeast including Victoria and the northern part of Tasmania from June–October [*Risbey et al*., 2009]. Finally, the intensity of the subtropical ridge (STR) has been noted to have important effects on winter precipitation in southern Australia [*Grose et al*., 2015].

Verdon-Kidd and Kiem [2009] argue that several of these drivers of precipitation have been differentially associated with the three major droughts of the past ~100 years, each of which had a distinct seasonal and spatial footprint. The Federation Drought (~1895–1902) exhibited spring-summer deficits and was associated with ENSO and the IPO [*Verdon-Kidd and Kiem*, 2009]. During the World War II (WWII) drought (~1937–1945), precipitation deficits were observed in all months, but the winter-spring deficits are consistent with the IOD being an important driver of this drought [*Verdon-Kidd and Kiem*, 2009]. Most recently, the Millennium Drought (or Big Dry, ~1997–2009), in which precipitation deficits were experienced in the autumn and early winter months, appears to have been driven by SAM [*Murphy and Timbal*, 2008; *Verdon-Kidd and Kiem*, 2009].

While regional drought conditions may provide a general indication of the hydroclimatic state, water resource managers are also interested in direct measures, such as streamflow, of the water moving into specific catchments. To date, relatively few streamflow reconstructions based on tree-rings have been developed in temperate regions for which precipitation is not strongly seasonal [but see, for e.g., *Lara et al*., 2008; *Mundo et al*., 2012], with most being for arid, semi-arid or Mediterranean climates. While long-term information is clearly required in these regions, there is also an urgent need for it in temperate areas that are heavily dependent on water resources, such as SEA. Not only is the area densely populated, but the Murray-Darling Basin (MDB; Figure 2) is a region of major agricultural importance for Australia. Furthermore, almost all of Australia's renewable hydroelectricity is generated in SEA and Tasmania produces ~60% of this. Although large impoundments in western and central Tasmania are used to generate hydroelectricity and supply water for agriculture and recreational purposes, water-intensive industries such as agriculture and hydroelectric production remain particularly vulnerable to extreme events such as drought or flood. This has recently been demonstrated by the very dry spring-autumn of 2015–2016 followed by severe flooding in June 2016 (http://www.energybusinessnews.com.au/business/infrastructure-news/no-end-in-sight-to-tassie-power-crisis/; http://www.abc.net.au/news/2016-06-09/mounting-tasmanian-damage-bill-feared-as-floodwaters-subside/7494504). Although model projections suggest that SEA will be increasingly subject to severe droughts and floods [*Hope et al*., 2015], considerable uncertainty surrounding these projections exists, particularly in relation to seasonal changes [*Chiew et al*., 2011; *Hope et al*., 2015]. Long palaeoproxy records can help to better place current conditions in a long-term context, and can also be used to improve calibration of climate models and hence reduce some of the uncertainty that currently exists around hydroclimate projections for SEA. However, to date most hydroclimatic reconstructions provide annual, not seasonal, records, limiting inference about how various climate drivers have interacted over long time scales to influence the distribution and amount of precipitation.

To partly address the lack of long and specifically seasonal records for SEA, *Allen et al*. [2015a] developed a reconstruction of December–January (early summer) hydroclimate for western Tasmania where several

large impoundments are located. Based on this reconstruction, it was found that recent summer conditions were well within historical variability and several periods of more prolonged and severe dry conditions have occurred in the past [*Allen et al*., 2015a]. This reconstruction did not, however, provide any information about the cool season, the period of the year during which the highest proportion of precipitation falls in western Tasmania. As such, a multicentennial cool season hydroclimate reconstruction would be particularly useful for understanding potential variation in water inflows into west Tasmanian catchments. For regions such as SEA that have quite strongly seasonally defined drivers of precipitation, a more detailed seasonal understanding of interseasonal variability in water availability over decades and centuries is critically important for developing resilient water management strategies and guiding policies and investment across many sectors of the economy [see *Holz et al*., 2010]. Therefore, hydrological reconstructions for multiple seasons will be enormously important in developing risk-based management tools for both agriculture and hydroelectricity production.

Here we present a tree-ring reconstruction of July–August dam inflows for Lake Burbury in western Tasmania using a mixture of new wood properties and ring width chronologies. This reconstruction complements our recent December–January inflow reconstruction for the same region [*Allen et al*., 2015a], thus enabling a comparison of cool and warm season hydroclimate over the past three centuries for western Tasmania. We also consider the degree to which our Tasmanian hydroclimate reconstruction matches recent hydroclimatic reconstructions for the agriculturally important MDB.

2. Materials and Methods

Exposed to the "Roaring 40s" winds, the mountainous western part of Tasmania typically receives up to 3 m of rain per year compared to the average 500–600 mm experienced on the eastern side of the island. As a consequence, several major water impoundments, primarily for the generation of renewable hydropower, have been constructed in the much wetter west. At approximately 556 km^2, Lake Burbury, located in the central west of Tasmania, lies between other major impoundments such as Lakes Gordon and Pedder to the south and Lakes Mackintosh and Murchison to the north (Figure 2). The construction of a dam over the King River in the late 1980s led to the formation of Lake Burbury. Tributaries from 11 rivers and creeks that originate in the Tasmanian World Heritage Area flow into the King River, and hence, Lake Burbury.

The King River streamflow gage directly measured flows into the basin from 1924 until 1990 after which changes in lake level and power station flow and spill have been used to directly estimate inflow. As a result, Lake Burbury has the longest and highest quality inflow record available for western Tasmania. Because of the size of Lake Burbury, the high-quality inflow data, and strong indications that flows in west Tasmanian catchments are closely related to one another other [*Allen et al*., 2015b] (supporting information Figure S1), we have focused our reconstruction efforts on inflow to Lake Burbury. Although the King River gage began operation in 1924, associated metadata indicate that the first 20 years of the record (1924–1944 for winter months) were generally low quality. A comparison with catchment-wide precipitation (Australian Water Availability Project AWAP 26h) [*Jones et al*., 2009a] likewise indicated a weak relationship prior to 1942 (data not shown). As a consequence, we have limited our analyses to the high-quality data from 1942 to the present for our model calibration and verification. A July–August (JA) streamflow index for western Tasmania (1942–2007) based on the average standardized scores of five rivers (supporting information Table S1) is also strongly associated with Lake Burbury inflows and King River streamflows (supporting information Figure S1).

We used a pool of 39 Tasmanian tree-ring chronologies (supporting information Table S2 and Figure S2) as potential predictors of inflow. These chronologies are based on ring width or other wood properties and come from four key species: *Athrotaxis cupressoides*, *Athrotaxis selaginoides*, *Phyllocladus asplenifolius*, and *Lagarostrobos franklinii*. The wood properties chronologies included density, cell wall thickness, tracheid radial diameter, and microfibril angle. These wood properties were measured using Silviscan3, a fast-assessment and high-resolution technology previously developed to characterize cellular scale variation in wood structure [*Evans*, 1994]. Density and cell diameter were measured at 25 μm intervals and cell wall thickness calculations derived from these two properties. Microfibril angle, the orientation of cellulose microfibrils in the secondary cell wall of wood cells and a sensitive indicator of environmental conditions [*Drew et al*., 2013], was measured at 100 μm intervals. In total, Silviscan analyses generated over five million

measurements that were then integrated into the wood properties chronologies used in the pool of potential predictors. Critically for this winter reconstruction, we have now been able to include mean earlywood and latewood properties chronologies (for density, cell diameter, cell wall thickness) in our pool of potential predictors. These earlywood and latewood properties were not available when our December–January reconstructions [*Allen et al*., 2015a] were developed, and we expected that they might contain information more applicable to the early or late growing season for each species. Standardization of tree-ring series aims to remove biological variability from tree-ring series. Density and cell wall thickness series were standardized using a negative exponential/regression line and both tracheid radial diameter and mirofibril angle series were standardized using the Friedman supersmoother [*Friedman*, 1984]. An age-dependent smoothing spline was used to standardize ring width series [*Melvin et al*., 2007]. We found that these standardization options resulted in the least trend distortion overall for the respective wood property types from these sites. All were standardized within a signal-free framework [*Melvin and Briffa*, 2008] and chronologies produced using residuals [*Cook and Peters*, 1997]. All of the chronologies spanned at least the AD1800 to 2007 period and only those portions of chronologies that contained at least five samples and had an Expressed Population Signal (EPS) [*Wigley et al*., 1984] ≥ 0.8 were used in our reconstructions. Details of individual ring width chronologies can be found in *Buckley et al*. [1997] and *Allen et al*. [2001, 2011, 2015b] and further details on the development of wood properties chronologies can be found in *Drew et al*. [2013].

We used a principal components regression approach [*Cook et al*., 2013] to reconstruct Lake Burbury July-August (JA) dam inflow. Both the tree-ring predictors and inflow data were prewhitened (autoregressively modeled) to ensure observations in both series were independent of one another prior to testing for relationships with inflow. All potential tree-ring predictors were then screened using a two-tail test, and only those significantly correlated with dam inflow ($p < 0.1$) were passed to the principal component regression (PCR) stage of the analysis. Autoregression was added back into the final reconstruction. We did not use lagged predictors in this analysis because we are reconstructing winter, not summer inflows and previous work has found significant lagged relationships only with the prior summer [*Allen et al*., 2001, 2011; *Buckley et al*., 1997; *Drew et al*., 2013]. The minimum Akaike Information Criterion (AIC) criterion was used to select the number of principal components used in the reconstruction regression model [see *Cook et al*., 1999]. The maximum entropy bootstrap which preserves the persistence structure present in the data [*Vinod and Lòpez-de-Lacalle*, 2009], was applied to both the tree-ring predictors and inflow (streamflow index) series prior to predictor selection, prewhitening and regression [see *Cook et al*., 2013], enabling production of 300 replicates of the reconstruction. This bootstrapping process produced an empirical probability distribution for each year, permitting estimation of uncertainty for each year in the reconstruction. The inflow reconstruction shown is based on the median of the boostrapped estimates. A further benefit of the bootstrapping process is that semiparametric uncertainty estimates for the calibration/verification statistics can also be calculated [*Cook et al*., 2013].

We used the longer 1963–2007 period for model calibration and withheld the 1942–1962 period for verification purposes. We used this longer calibration period in order to capture as much of the range of variability in the calibration period as possible to try to avoid the "no-analogue problem" [*Fritts and Swetnam*, 1989]. The calibrated models were assessed using R^2 (CRSQ), the classical measure of the goodness of model fit in regression models, and the cross-validation reduction of error (CVRE) calculated using a leave-one out procedure. For the verification period, Pearson's R^2 (VRSQ) provided a measure of the goodness of model fit, and the reduction of error (VRE) and coefficient of efficiency (VCE) were used to assess whether the calibrated model verified. Both VRE and VCE range between $-\infty$ and 1 and any positive value of these statistics indicates model skill. The coefficient of efficiency (VCE) is the most rigorous of these statistics. More detail about these commonly utilized statistics can be found in *Cook et al*. [1999]. A nonparametric sign test was also applied to further assess interannual agreement between the Hydro inflow data and the reconstruction. We did this in two different ways. First, we examined whether the anomalies of the two series were on the same side of the mean. Second, we examined whether the sign of first differences for each year was the same for both series.

To place our reconstruction in a broader geographical context, we also identified the spatial extent of relationships between Tasmanian flow data (Lake Burbury inflow and the west Tasmanian streamflow index) and mainland Australian streamflow. We selected mainland streamflow records extending back to at least

1960 from the Bureau of Meteorology's (BOM) reference network (www.bom.gov.au) in Victoria (VIC) and New South Wales (NSW; see Figure 2). Unfortunately, a lack of reference stations further inland (www.bom.gov.au) meant we were unable to test relationships between Tasmanian flow records and streamflow in the more arid interior of the MDB. We also examined the relationship between both the Lake Burbury inflow data and the inflow reconstruction and each of: gridded GPCCv7 precipitation, mean sea level pressure (MSLP; 20th Century reanalysis), and sea surface temperature (20th Century reanalysis). These analyses were done with Climate Explorer (https://climexp.knmi.nl) [*Trouet and van Oldenborgh*, 2013].

We compared our verified reconstruction with three phenomena previously linked with west Tasmanian winter precipitation and streamflow [*Risbey et al*., 2009; *Allen et al*., 2015b]: the SAM, IOD, and STR. The seasonal Fogt index for SAM [*Jones* et al., 2009b] is available at: http://polarmet.osu.edu/ACD/sam/sam_recon.html) and Martin Visbeck kindly provided his monthly SAM index [see *Visbeck*, 2009]. The IOD index data are available at http://gcmd.nasa.gov/records/GCMD_Indian_Ocean_Dipole.html. We used an updated version of *Drosdowsky*'s [2005] STR intensity (DSTR-I) calculated for eastern Australia only and also *Larsen and Nichols*' [2009] STR index of intensity (LSTR-I) averaged over longitudes 135°–150°E. Although the influence of the subtropical IOD (SIOD) has been discussed for southwestern Western Australia [*England et al*., 2006], it has not been explored for southeastern Australia. We therefore also examined the relationship between this index and our reconstructions (data sourced from https://climexp.knmi.nl).

3. The Inflow Reconstruction

Only three tree-ring chronologies from western Tasmania were selected as predictors in the verified dam inflow reconstruction (Figure 2 and Table 1). The predictors included Mt Read (MRD) and Reservoir Lakes (RL), both *Athrotaxis selaginoides* tree-ring width sites, and Tyenna *Phyllocladus aspleniifolius* (latewood cell wall thickness; TNELWWT; see Table 1). *Allen et al*. [2001, 2011; *Allen*, 2002] have previously noted strong relationships between some tree-ring sites and winter climate for both *Phyllocladus aspleniifolius* and *Athrotaxis selaginoides*, but the same has not been found for *Lagarostrobos franklinii* or *Athrotaxis cupressoides* [*Buckley et al*., 1997; *Allen et al*., 2011]. The selection of the above sites is therefore consistent with previous evidence of cool season relationships in these species at some sites. It is worth noting that neither of these ring-width series were selected as predictors in the previous December–January reconstruction [*Allen et al*., 2015a]. Correlations between individual predictors for the JA reconstruction and inflow are moderate, varying between |0.289| and |0.358| (Table 1). The relative influence of each chronology included in an individual reconstruction can be captured as a percentage of the sum of the absolute values of the beta weights of all predictor chronologies used in that reconstruction [*Frank and Esper*, 2005]. Here, influence is heavily weighted toward the TNE LWWT chronology (57.5%; Table 1).

Table 1. Tree-Ring Chronologies Used in Reconstruction, 1731–2007[a]

Predictor	Period of Chronology Used ($n > 5$, EPS ≥ 0.8)	Corr	Beta	Weight (%)
Mt Read King Billy Pine ring width (MRD) (*Athrotaxis selaginoides)*	1710–2007	−0.289	−0.43	21.2
Reservoir Lake King Billy Pine ring width (RL) (*Athrotaxis selaginodies)*	1710–2007	−0.315	−0.433	21.3
TNE average latewood cell wall thickness (TNE LWWT) *(Phyllocladus aspleniifolius)*	1731–2007	−0.358	−1.169	57.5

[a]Site name and abbreviation (in parentheses) given. The Cor column shows correlations between July–August inflow and predictors used in the reconstruction. The Beta column reports Beta weights for the initial reconstruction model based on all predictors (1716–2007). The weights are percentages and provide an indication of the influence of individual predictors on the final reconstruction. Note that the TNE site name is based on the Forestry Tasmania coupe number. VCE point estimate > 0 back to 1710, but interval estimate of VCE > 0 since 1731 only.

While the point estimate for VCE > 0 from 1710, the interval estimate of VCE only exceeded 0 after 1731 (Table 2). Although median calibrated (0.216 [0.108–0.282]) and verified (0.246 [0.191–0.315]; Table 2 and Figure 3) variance is relatively low compared to several hydrological reconstructions elsewhere [e.g., *Brito-Castillo et al*., 2003; *Woodhouse et al*., 2006; *Gou et al*., 2007; *Akkemik et al*., 2008; *Stahle et al*., 2011; *Cook et al*., 2013; *Pederson et al*., 2013 among numerous others], it is very similar to that reported *Gallant and Gergis* [2011] for reconstructed Murray River flow and more than twice that reported by *Tozer et al*. [2016] for their Williams River reconstruction further north along the NSW

Table 2. Calibration and Verification Statistics for AD 1731–2007 of the Median Reconstruction Based on 300 Bootstrapped Replicates[a]

Statistic	L Burbury Reconstruction
CRSQ	0.216 (0.108,0.282)
VRSQ	0.246 (0.191,0.315)
CVRE	0.13 (0.028,0.208)
VRE	0.248 (0.174,0.318)
VCE	0.228 (0.154,0.299)
Sign test (anomlies)	44, 21 ($p < 0.01$)
Sign test (first differences)	47, 18 ($p < 0.01$)

[a]Figures in parentheses show the non-parametric 90% intervals for the statistics. CRSQ is R^2 for the calibration period, VRSQ is R^2 for the verification period, CVRE is the leave-one-out cross-validation reduction of error for the calibration period; VRE is the RE statistic for the verification period, and VCE is the CE statistic for the verification period. The sign test shows the number of agreements in the sign of the reconstruction and the Hydro inflow data for Lake Burbury. Both the sign of anomalies and the sign of first differences were tested. The first number shown in each pair is the number of agreements in sign, the second is the number of disagreements. *p* Values derived from the normal approximation to the binomial distribution.

coast. Additionally, we are relying on the interval, rather than the point, estimates of VRE and VCE, to assess our reconstructions of cool season hydroclimate. Our reconstruction therefore uses a stricter measure of skill than that applied in several other Australian hydroclimatic reconstructions [e.g., *McGowan et al*., 2009; *Vance et al*., 2014*; Tozer et al*., 2016]. Further, both sign tests indicate significant similarity ($p < 0.01$), between the Lake Burbury inflow data and the reconstruction, consistent with the rigorous VRE and VCE statistics. So, while our reconstruction does not approach the quite high levels of variance in flow explained in other studies (often in excess of 40%), it is comparable with other hydroclimate reconstructions for SEA. These reconstructions all demonstrate the greater difficulty inherent in developing hydrological reconstructions from proxies in temperate regions where water is not a strongly limiting factor for tree growth.

Overall, the reconstruction indicates that JA inflows for the last two decades are well within the variability of the past 277 years (Figures 3b and 3c). The reconstruction indicates periods of low inflows in the 1860s, early1900s, and around 1970 (Figures 3a and 3b), but relatively high inflows in the 1770s and 1810s. After 1850, greater decadal frequency variability in the series is apparent (Figure 3c) although this is not strongly indicated in the series wavelet (Figure 3d). In addition, there are no peaks of the same magnitude as those centered on the 1770s and 1810s after the 1810s (Figure 3c). An examination of median inflow and variability in the reconstruction for successive 25 year periods indicates median inflow for each quarter-century was close to the long-term median inflow (Figure 4). Variability was generally higher from about 1825–1925 than for other periods. In general, the number of positive outliers is greater than the number of negative outliers. Streamflow data are commonly positively skewed, especially for short intervals of time, so a greater number of positive outliers for a period that covers two calendar months is not surprising. Inflows in the first quarter of the 20th century were distinctly negatively skewed due to the low reconstructed flows in 1909 (see below). Interestingly, median inflows for the last two 25 year periods of the 20th century (and the shorter 7 year period since 2000) were below the long-term median (Figure 4).

Although the moderate explanatory power of our reconstruction means analysis of low-frequency variability is more likely useful than analysis at the interannual level, a brief examination of how extreme flow years align with documentary or instrumental records may help highlight relative strengths and weaknesses of the reconstruction. The five highest single-year JA inflow events in the reconstruction (starting with the wettest) are: 1816, 1776, 1828, 1745, and 1964 whereas the five wettest years in the instrumental record (starting with wettest) are: 1946, 1970, 1964, 1992, and 1955. Two of the wettest years in the reconstruction occur the year after major volcanic eruptions (1816 and 1964) and additional discussion of this is contained in the supporting information and references therein (S4) [*Anchukaitis et al*., 2010; *Buckley et al*., 2010; *Chenoweth*, 1996; *Gao et al*., 2008; *Jiayu*, 1992; *Oppenheimer*, 2003; *Palmer and Ogden*, 1992; *Schmidt et al*., 2011; *Trigo et al*., 2009; *Villalba* and *Boninsegna*, 1992; *Wilson*, 1992]. This discussion includes the results of a superposed epoch analysis using *sea* function in dplR [*Bunn et al*., 2015]. The five lowest reconstructed inflow events (starting with the driest) are: 1909, 1954, 1935, 1868, and 1919, compared with 1957, 1950, 1982, 1989, and 1987 in the instrumental record. Using the information from the hat matrix [*Haoglin and Welsh*, 1978], we identified the wettest (1816) and driest (1909) reconstructed years as extrapolations because the lower confidence limit for these years based on the 300 reconstructions exceeded the threshold for extrapolation. Although this reflects the fact that the 1963–2007 calibration period did not include individual years with conditions as extreme as those reconstructed for 1816 and 1909, it is encouraging that

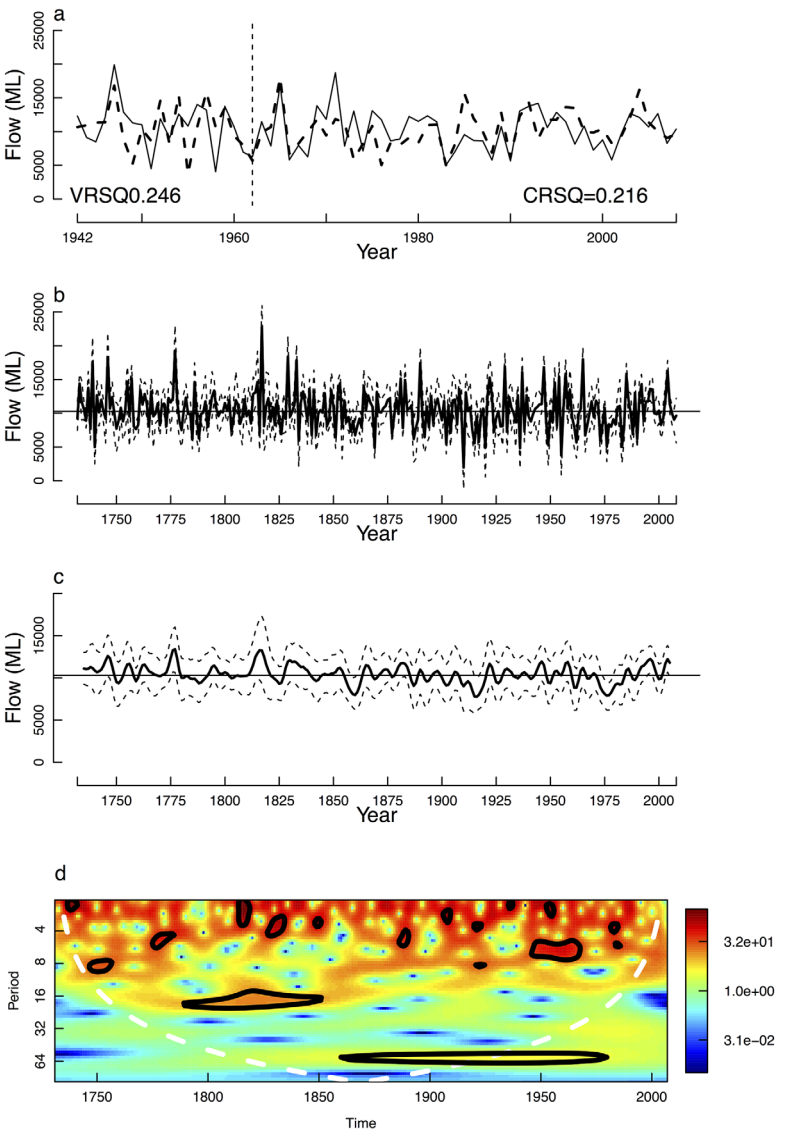

Figure 3. (a) The verified inflow reconstruction, 1942–2007, showing CRSQ and VRSQ. Solid line is Lake Burbury inflow data, and dashed line is reconstructed inflow; (b) Inflow reconstruction with 90% semiparametric bootstrapped intervals; (c) Smoothed reconstruction and 90% semiparametric bootstrapped intervals. A 7-year Gaussian smooth was used; (d) Wavelet for reconstructed inflow. Significant ($p < 0.1$) peaks occur throughout the reconstruction in the ~0–8 year band and there is a peak in power at ~16 years in the first half of the nineteenth century and a lower-frequency peak from around 1850 to late C20th, although this peak is less robust after ~1925 due to edge effects.

only inflows for two individual years were extrapolations. Documentary evidence points to unusual climate conditions in 1816 in particular, but also in some of the other key years noted above. The year 1816 was a wet year for the fledging NSW colony (Sydney) further north [*Gergis and Ashcroft*, 2013]. In June 1816, the Hawkesbury River flooded and in July prolonged gale conditions were responsible for two ships being wrecked and another being forced out to sea for a week [*Callaghan and Helman*, 2008]. Wet conditions persisted into the summer of 1816/1817 [*Fenby and Gergis*, 2013; *Palmer et al*., 2015]. *Evans* [2012] documented flooding in both the north and south of Tasmania in July–August 1816. Documentary records also indicate that flooding occurred in both northern and southern Tasmania over the 1828 July–September period [*Evans*, 2012], and that gales and floods occurred in northern/northwestern Tasmania in July and August of 1964 [*Evans*, 2012]. The gridded AWAP data [*Jones et al*., 2009a; www.csiro.au/awap] that extends back to 1901 also indicates that western Tasmania experienced rainfall in ~85th–90th percentiles for both July and August of 1964. Because 1745 and 1776 preceded European settlement, no documentary records for those

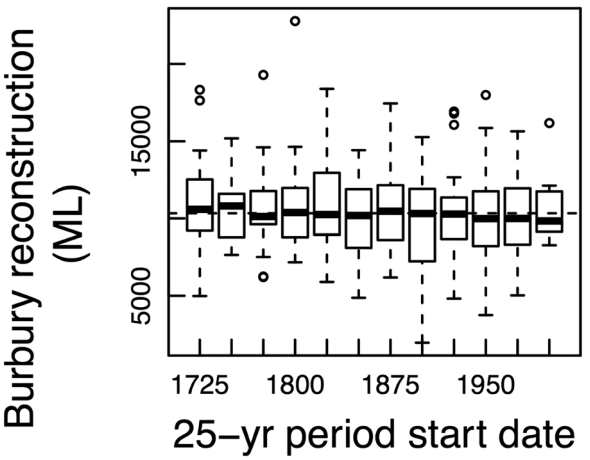

Figure 4. Successive 25 year periods of inflow reconstruction presented as box and whisker plots. Whiskers show the 10th and 90th percentiles and circles indicate outliers. The dashed horizontal line shows the overall median of the reconstruction.

years exist. However, 1745 commonly occurs as a very narrow ring in *Athrotaxis* spp. chronologies from northern Tasmania (unpublished data). Given the negative relationship between the ring-width chronologies and inflow (Table 1), a narrow ring would be consistent with high inflows.

Low inflow years in the reconstruction are less consistent with documentary and instrumental evidence. Although *Evans* [2012] describes the 1908–1910 period as one of drought in Tasmania, she also notes floods for June and August of 1909. The AWAP precipitation data, however, indicates that July was dry in the west and southwest of the state. The AWAP data also indicate that July1954 was somewhat dry in the southwest but around average over the central west and that wetter than average conditions occurred in August. There is also an obvious difference between the inflow data and reconstruction for 1954 (Figure 3a). Near average conditions occurred in 1935 and 1948 (www.csiro.au/awap/). *Evans* [2012] notes that drought persisted from August to December in 1919 in the state's south, but floods and snow in southern Tasmania were reported for July of 1868. Of the three major droughts experienced in the 20th century (Federation, WWII and the Millennium Drought), only the WWII drought (∼1937–1945) exhibited relatively large winter precipitation deficiencies in southern Australia, but this drought did not have a pronounced effect on western Tasmania [*Verdon-Kidd and Kiem*, 2009]. Therefore, none of these three major droughts of the past ∼110 years provide useful comparisons with our July–August reconstructions. Based on the available evidence presented here, our reconstruction appears to have greater fidelity for extreme wet years than extreme dry years. This contrasts with dendrohydrological studies elsewhere in which dry years/period are better reconstructed than wet years, and is a somewhat unexpected result. The reasoning for the under-prediction of high flows in river flow reconstructions is straight-forward. Tree growth has a saturated response to soil moisture availability; once a tree has adequate moisture, additional moisture will not induce additional growth. *Elshorbagy et al*. [2016] also point out that trees may not respond to flash floods or high runoff after drought conditions unless soil moisture remains high for extended periods. However, in our results, a narrow ring, or low cell wall thickness in the chronologies is associated with wet conditions, most likely reflecting the mesic environment in which these trees are growing. The heavy cloud cover and low light availability associated with wet conditions in western Tasmania can persist for weeks or months during the cool season and can inhibit photosynthesis [*Read and Busby*, 1990]. In addition, excess soil moisture may limit oxygen uptake by fine roots and restrict physiological activities of the tree [*Ruark et al*., 1983; *Parent et al*., 2008]. Further information regarding the growth response of these trees to climate is clearly needed. High-resolution dendrometer and climate data currently being collected from a number of Tasmanian species will help to better understand the climate response of the Tasmanian trees.

4. The Spatial Footprint of the Reconstruction and Relationship With the Murray-Darling Basin

Strong significant relationships between the Lake Burbury inflow (streamflow index) data and selected mainland Australian reference streamflow stations (Figures 5a and 5b) are consistent with a strong positive relationship between the Lake Burbury inflow data and the gridded GPCCv7 precipitation over the far south of mainland Australia (Figure 5c), and confirm strong positive relationships between instrumental data sets in these regions. Climatologically, this also makes sense because frontal rain (rain produced by the forcing of warm air over cold air), which is very important for western Tasmania, also accounts for significant precipitation over the Australian Alps and southwestern Victoria [*Risbey et al*., 2013]. The strong negative

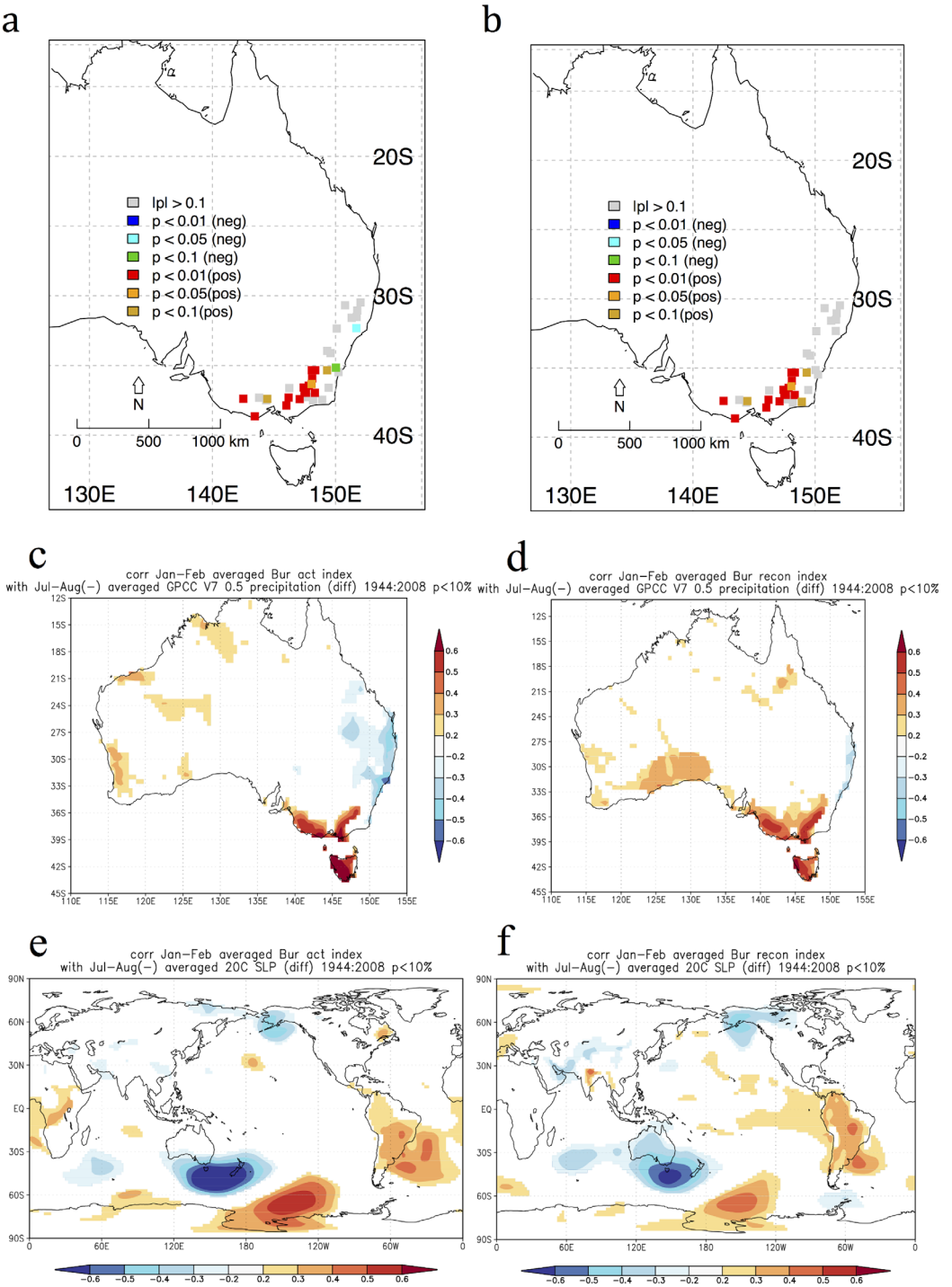

Figure 5. (a) Correlations between July–August Hydro Lake Burbury inflow and selected BOM hydrologic reference streamflow gage data. (b) Correlations between the west Tasmanian July–August streamflow index (S1) and selected BOM hydrologic reference streamflow gage data. Gage data from Victoria and NSW were selected on the basis that it extended back to at least 1960. (c) Correlation between Lake Burbury inflow and GPCC V7 precipitation over Australia 1942–2007. (d) As for Figure 5c, but with reconstructed Lake Burbury inflow. (e) Correlations between 20th Century Reanalysis MSLP and Lake Burbury July–August inflow, 1942–2007. (f) As for Figure 5e., but with reconstructed Lake Burbury inflow. Plots in Figures (c)–(f) constructed using KMNI data explorer (https://climexp.knmi.nl). *All data were first differenced to remove trend prior to calculation of correlations.*

relationship between the inflow data and rainfall along the central portion of the east coast (Figure 5c) is somewhat consistent with two significant negative associations ($p < 0.1$) between Lake Burbury inflow and streamflow in central coastal NSW (Figure 5a).

Although the spatial relationship between the reconstruction and SEA precipitation is generally weaker than that between precipitation and the Lake Burbury inflow data, the spatial patterns of the two are remarkably coherent (Figures 5c and 5d). The inability of our reconstructions to capture the negative relationship between precipitation and inflows over the central east coast of the continent shown in the instrumental data is most likely related to the greater sensitivity of the Tasmanian trees to conditions in Tasmania rather than those farther afield. The patterns shown in Figure 5 suggest that our reconstruction will not be particularly useful as an indication of past winter conditions in the MDB because strong relationships are to the south of the MDB (Figures 5a–5d). It may, however, be useful for examining long-term flows to the south of the basin. Nevertheless, it is instructive to compare our reconstruction with *Gallant and Gergis*' [2011] annual Murray River streamflow reconstruction (August–July) and the annual (July–June) reconstruction for the Upper Murray Basin [*Ho et al*., 2015]. The Lake Burbury inflow reconstruction is generally mismatched with both these reconstructions, and it does not strongly reflect *McGowan et al*.'s [2009] wetter and drier periods (supporting information Figure S3). Nonetheless, all reconstructions indicate wetter than average conditions around 1880 and 1950s and drier than average conditions around 1885 and 1900.

The general lack of fit between our reconstruction and other reconstructions for the River Murray is hardly surprising for two main reasons. First, the MDB region reconstructions are based on MDB flows, and as shown in Figures 5a–5d, strong positive relationships between southern Australia's hydroclimate and our inflow reconstruction extend only as far as the southern boundary of the MDB. This is also the case for the instrumental inflow data. Second, all three other reconstructions have focused on annual flows (albeit for slightly different windows) while our reconstruction is specifically for JA inflows in western Tasmania. The JA Lake Burbury inflow data are not a particularly good reflection of annual inflow to the basin (r ~0.57 for both January–December and October–September). Different ocean-atmosphere processes that drive seasonal precipitation and significant precipitation in other seasons will be largely responsible for this, as explained briefly in the Introduction and elaborated upon elsewhere [e.g., *Hendon et al*., 2007; *Risbey et al*., 2009]. Greater variability in both the *Ho et al*. [2015] and *Gallant and Gergis* [2011] reconstructions than in the Lake Burbury reconstruction may also reflect different drivers of precipitation over these areas. For example, several studies have linked the hydroclimate of the MDB region with ENSO and/or the low frequency oscillation of the IPO [*Verdon et al*., 2004; *McGowan et al*., 2009; *Gallant and Gergis*, 2011; *Palmer et al*., 2015], whereas there were no significant relationships between either the SOI or IPO and our reconstruction (data not shown). Further, spatial correlations of our reconstruction with MSLP (Figures 5e and 5f) are not typical of the IPO MSLP signature [*Henley et al*., 2015]. Instead, the strong negative correlations with MSLP over southern Australia for both the instrumental Lake Burbury inflow data and the reconstructed inflow (Figures 5e and 5f) are consistent with observations that relationships between MSLP and precipitation in the extratropics are typically negative. The broader pattern (Figures 5e and 5f) may suggest atmospheric blocking (J. Risbey CSIRO, personal communication 2016). A third reason for poor relationships with MDB reconstructions may be the moderate strength of all these reconstructions, including our JA reconstruction. Spatial correlations between the inflow reconstruction and SSTs were weak and showed no particular pattern (data not shown).

Table 3. Correlations Between Various Indices (see text) and the Lake Burbury Inflow Reconstruction[a]

Index	Burbury Recon (Common Period)	Burbury Recon 1942–2007	Burbury Inflow 1942–2007
IOD	−0.38**		−0.18
SIOD	−0.42**		−0.22
SAM (V)	0.03	−0.02	−0.20*
SAM(SR)	−0.16	−0.31**	−0.58**
DSTR-I	−0.3**	−0.40**	−0.25*
LSTR-I	−0.28*	−0.39**	−0.27**

[a]All data were detrended prior to computing correlations. SAM (V) is the Jul–August Visbeck index of SAM; SAM(SR) is the seasonal SAM reconstruction; STRI(D) is the Drosdowsky index of subtropical ridge intensity and STRI(L) is the Larsen and Nichols index of subtropical ridge intensity. A *Indicates statistical significance at $p \leq 0.05$ and **Indicates statistical significance at $p \leq 0.01$. (common period) indicates correlations were calculated for the period in common between the reconstruction and each of the indices.

We found a strong correlation between the JA instrumental inflow data for Lake Burbury and winter SAM (−0.58; Table 3), but the correlation with reconstructed inflow was considerably weaker (−0.31 for the 1942–2007 period and −0.16 for the 1905–2007 period; Table 3). Significant, but relatively weak, relationships between the reconstruction and the two STR indices also exist (DSTR-I:−0.3 to −0.4; and LSTR-I: −0.28 to −0.39; Table 3). Correlations with the instrumental data were weaker, but reasonably comparable (−0.25 and −0.27). Significant relationships between the Lake Burbury reconstruction and each of the SIOD (−0.42)

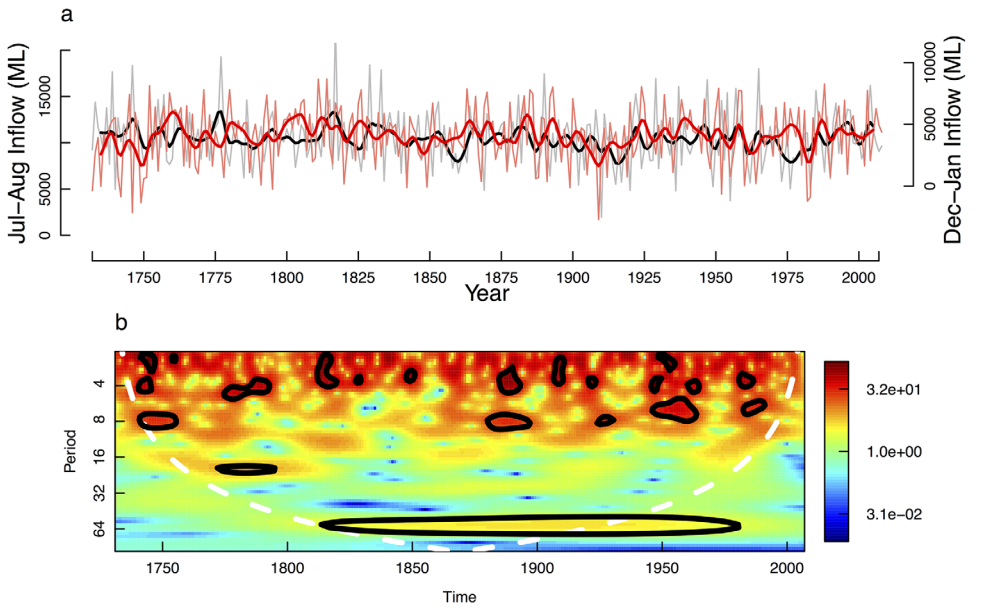

Figure 6. (a) Comparison of *Allen et al.*'s [2015] reconstructed December–January inflow (red) with reconstructed July–August reconstruction (black) for Lake Burbury. Thick lines show 7 year Gaussian smoothing for the respective seasons. Correlation between the two unsmoothed series is −0.04 (summer to winter) or 0.11 (winter to summer). (b) Wavelet coherence of the two reconstructions over their common period. Highest power is at periods lower than 8 years.

and IOD (−0.38) were less consistent with those with the Lake Burbury inflow data (−0.18 and −0.22 respectively; Table 3). Overall, these results are broadly consistent with previous work [e.g., *Risbey et al.*, 2009].

5. Comparison of December–January and July–August Inflow at Lake Burbury

Distinct seasonal expression of past droughts [e.g., *Verdon-Kidd and Kiem*, 2009] suggests that both drought and pluvial signals in the DJ Lake Burbury inflow reconstructions [*Allen et al.*, 2015a] are likely to differ from those in the JA reconstruction. Other questions about the relationship between the two reconstructions include: have there been changes in the relationship between the seasons over time? Are there clear periods when both reconstructions indicate wet (dry) conditions or are they typically mismatched?

There is a general mismatch between the DJ and JA instrumental inflow data ($r = -0.04$ summer to winter and 0.11 winter to summer) that is reflected in the DJ and JA Lake Burbury reconstructions (Figure 6a; $r = -0.08$ summer to winter and $r = -0.05$ winter to summer). One clear visual example of mismatch in the reconstructions is relatively high winter inflows in the 1770s that do not correspond with relatively high summer inflows (Figure 6a). However, the generally high winter inflows in the 1810s are somewhat consistent with relatively high summer inflows for the same period (Figure 6a). Wavelet coherence of the two reconstructions (Figure 6b) shows periods of significant coherence in the 2–8 year band, primarily before 1800 and then again from the late 1800s into the 20th century. Differences between our two seasonal reconstructions (and the instrumental data itself) for the same region, and suggested changes in the relationship in the frequency domain over time, point to the importance and relevance of seasonal reconstructions when drivers of precipitation differ on a seasonal basis, and when relationships between seasons vary over time. Future work to improve reconstructed flows for SEA will better enable interseasonal comparisons.

6. Conclusions

Information about low-frequency variability in the hydroclimate of southeastern Australia is sorely needed to help improve water resources management in this heavily populated and important agricultural region. Furthermore, given the seasonal nature of major ocean-atmosphere processes driving precipitation and drought in this region, an understanding of interseasonal variations over long time scales is critically

important for planning purposes. This low-frequency information cannot be readily resolved from the short instrumental record. Although hydrological reconstructions based on proxies such as tree-rings in temperate regions are unlikely to explain the levels of variance in arid and semi-arid regions, multiple competing demands for water in these regions makes temperate region reconstructions just as important and urgently needed.

While our reconstruction, the first specifically for the cool season in far southeastern Australia, is preliminary, it is nevertheless a vital step toward the development of robust and seasonally explicit hydrological reconstructions for the region. Our July–August reconstruction suggests that recent winter dam inflows for individual years are well within the range of variability over the last three centuries. However, although the wettest events in the reconstructed record since the 1803 European settlement of Tasmania are well corroborated by multiple historical records, low flow events are not well captured. The lack of strong links between our inflow reconstruction and several Murray River streamflow reconstructions, as well as poor relationships between actual streamflow data for Tasmania and the coastal southeastern mainland north of the Australian Alps, cautions against using a single reconstruction to represent conditions across the whole of SEA. Indeed, it is more fitting to view our reconstruction as complementary to those for the MDB, because it is more strongly related to the area south of the basin, reflecting different impacts of various ocean-atmosphere processes on precipitation over the broader region.

Further improvements in the seasonal reconstructions will facilitate more detailed explorations of changes in the seasonal distribution of precipitation that will be especially pertinent for production of renewable hydroelectricity. Based on our experience, additional ring-width chronologies—at least from the long-lived Tasmanian species—are unlikely to yield the required improvements in tree-ring-based hydrological records for this region. Rather, nontraditional tree-ring chronologies such as tracheid radial diameter, microfibril angle, cell wall thickness, and early/latewood derivatives of these are likely to underlie further improvements in the tree-ring-based hydrological reconstructions for this region. Incorporation of other types of highly resolved but local proxies (e.g., some speleothems can be highly resolved) [*Ho et al*., 2015] may be another avenue for improvement, albeit a more complex one.

The very dry conditions in Tasmania from spring 2015 to autumn 2016, and decisions made concerning the management of the water resources over this period, highlight the relevance of multicentennial records of seasonal variability. Our preliminary, but seasonally targeted reconstructions for this region where distinct wet and dry seasons do not exist are a critical step towards providing the much-needed multicentennial hydrological records.

Acknowledgments

Dam inflow data for this study are available from Hydro Tasmania and the inflow reconstruction can be obtained from the corresponding author. Tree-ring data used in this reconstruction are archived at the International Tree Ring Data Bank (ITRDB: www.ncdc.noaa.gov). We thank Amy Hessl, Holly Faulstich, Rohan Simkin, and Jason Rijnbeek for assistance in the field. Mark Willis, Hydro Tasmania, provided descriptive data about the catchments used in this study. Ailie Gallant kindly provided the Murray River reconstruction and Wasyl Drosdowsky and Stuart Larsen provided their respective indices of the STRI. We also thank James Risbey for comments on the spatial correlation patterns, and three anonymous reviewers for their thoughtful comments and suggestions that have substantially helped to improve this paper. Samples for this study were obtained under permits issued by Forestry Tasmania and Parks and Wildlife Tasmania. Bill Cohen from Hydro Tasmania provided the catchment map and Michelle Ho and Tom Fairman also assisted with the maps. K.A. and S.N. were supported by an Australian Research Council Linkage Project (LP12020811) cofunded by Hydro Tasmania. P.J.B. was supported by Australian Research Council Future Fellowship FT120100751. This paper is also Lamont-Doherty Earth Observatory contribution 8080.

References

Akkemik, U., R. D'Arrigo, P. Cherubini, N. Köse, and G. C. Jacoby (2008), Tree-ring reconstructions of precipitation and streamflow for northwestern Turkey, *Int. J. Climatol.*, *28*, 173–183.

Allan, R. (1988), El Niño Southern oscillation influences in the Australasian region, *Prog. Phys. Geogr.*, *12*, 313–348.

Allen, K. J., E. R. Cook, R. J. Francey, and K. Michael (2001), The climatic response of *Phyllocladus aspleniifolius* (Labill.) Hook. F. in Tasmania, *J. Biogeogr.*, *28*, 305–316.

Allen, K. J. (2002), The temperature response in the ring widths of *Phyllocladus aspleniifolius* (Celery-top Pine) along an altitudinal gradient in the Warra LTER Area, Tasmania, *Aust. Geogr. Stud.*, *40*, 287–299.

Allen, K. J., J. Ogden, B. M. Buckley, E. R. Cook, and P.J. Baker (2011) The potential to reconstruct broadscale climate indices associated with Australian droughts from Athrotaxis species, Tasmania, *Clim. Dyn.*, *37*, 1799–1821.

Allen, K. J., S. C. Nichols, R. Evans, E. R. Cook, S. Allie, G. Carson, F. Ling, and P. J. Baker (2015a), Preliminary December-January inflow and streamflow reconstructions from tree-rings for western Tasmania, southeastern Australia, *Water Resour. Res.*, *51*, 5487–5503, doi: 10.1002/2015WR017062.

Allen, K. J., G. Lee, F. Ling, S. Allie, M. Willis, and P. J. Baker (2015b), Palaeohydrology in climatological context: Developing the case for use of remote proxies in Australian streamflow reconstructions, *Appl. Geogr.*, *64*, 132–152.

Allen, W. (1895), The droughts and floods of Australia, *Morning Bulletin Rockhampton*, 19 August 1895.

Anchukaitis, K. J., B. M. Buckley, E. R. Cook, R. D. D'Arrigo, and C. M. Ammann (2010), Influence of volcanic eruptions on the climate of the Asian monsoon region, *Geophys. Res. Lett.*, *37*, L22703, doi:10.1029/2010GL044843.

Brito-Castillo, L., S. Dìaz-Castro, C. A. Salinas-Zavala, and V. Douglas (2003), Reconstruction of long-term winter streamflow in the Gulf of California continental watershed, *J. Hydrol.*, *278*, 39–50.

Buckley, B. M., E. R. Cook, M. J. Peterson, and M. Barbetti (1997), A changing temperature response with elevation for *Lagarostrobos franklinii* in Tasmania, Australia, *Clim. Change*, *36*, 477–498.

Buckley, B. M., K. J. Anchukaitis, D. Penny, R. Fletcher, E. R. Cook, M. Sano, L. Nam, A. Wichienkeeo, T. Minch, and T. Hong (2010), Climate as a contributing factor in the demise of Angkor, Cambodia, *Proc. Natl. Acad. Sci. U. S. A.*, *107*, 6748–6752.

Bunn, A., M. Korpela, F. Biondi, F. Campelo, P. Mérian, F. Qeadan and C. Zang (2015), *dplR: Dendrochronology Program Library in R. R package version 1.6.3*. [Available at http://CRAN.R-project.org/package=dplR.]

Cai, W., P. van Rensch, S. Borlace, and T. Cowan (2011), Does the Southern Annular Mode contribute to the persistence of the multidecade0long drought over southwest Western Australia? *Geophys. Res. Lett.*, *38*, L14712, doi:10.1029/2011GL047943.
Callaghan, J., and P. Helman (2008), *Severe Storms on the East Coast of Australia 1770–2008*, Griffith Cent. for Coastal Manage. and Griffith Clim. Response Program.
Chenoweth, M. (1996), Ships' logbooks and "The year without a summer" *Bull. Am. Meteorol. Soc.*, *77*, 2077–2093.
Chiew, F. H. S., W. J. Young, W. Cai, and J. Teng (2011), Current drought and future hydroclimate projections in southeast Australia and implications for water resources management, *Stochastic Environ. Res. Risk Assess.*, *25*, 601–612.
Cook, E. R., and K. Peters (1997), Calculating unbiased tree-ring indices for the study of climatic and environmental change, *Holocene*, *7*, 361–370.
Cook, E. R., D. M. Meko, D. W. Stahle, and M. K. Cleaveland (1999), Drought reconstruction for the continental United States, *J. Clim.*, *12*, 1145–1162.
Cook, E. R., J. G. Palmer, M. Ahmed, C. A. Woodhouse, P. Fenwick, M. U. Zafar. M. Whab, and N. Khan (2013), Five centuries of Upper Indus flow from tree rings, *J. Hydrol.*, *486*, 366–375.
Cullen, L. E., and P. F. Grierson (2009), Multi–decadal scale variability in Autumn–Winter rainfall in south–western Australia since 1655 AD as reconstructed from tree–rings of *Callitris columellaris*, *Clim. Dyn.*, *33*, 433–444.
Drew, D. M., K. J. Allen, G. M. Downes, R. Evans, M. Battaglia, and P. J. Baker (2013), Wood properties in a long–lived conifer reveal strong climate signals where ring width series do not, *Tree Physiol.*, *33*, 37–47.
Drosdowsky, W. (1993), An analysis of Australian seasonal rainfall anomalies: 1950–1987. II: Temporal variability and teleconnection patterns, *Int. J. Climatol.*, *13*, 111–149.
Drosdowsky, W. (2005), The latitude of the subtropical ridge over eastern Australia: The L index revisited, *Int. J. Climatol.*, *25*,1291–1299.
Elshorbagy, A., T. Wagener, S. Razavi, and D. Sauchyn (2016), Correlation and causation in tree-ring based reconstruction of paleohydrology in cold semi-arid regions, *Water Resour. Res.*, *52*, doi:10.1002/2016WR018985.
England, M. H., C. C. Ummenhofer, and A. Santoso (2006), Interannual rainfall extremes over southwest Western Australia linked to Indian Ocean climate vulnerability, *J. Clim.*, *19*, 1948–1969.
Evans, K. (2012), 'Antipodean England'? A History of Drought, Fire and Flood in Tasmania from European Settlement in 1803 to the 1960s, PhD thesis, Sch. of Geogr. and Environ. Stud., Univ. of Tasmania.
Evans, R. (1994), Rapid measurement of the transverse dimensions of tracheids in radial wood sections from *Pinus radiata*, *Holzforschung*, *48*, 168–172.
Fenby, C., and J. Gergis (2013), Rainfall variations in south-eastern Australia part 1: Consolidating evidence from pre-instrumental documentary sources, 1788–1860, *Int. J. Climatol.*, *33*, 2956–2972.
Frank, D., and J. Esper (2005), Temperature reconstructions and comparisons with instrumental data from a tree-ring network for the European Alps, *Int. J. Climatol.*, *25*, 1437–1454.
Friedman, J. H. (1984), A variable span scatterplot smoother, *Standford Univ. Tech. Rep. 5*, Standford, Calif.
Fritts, H. C., and T. W. Swetnam (1989), Dendroecology: A tool for evaluating variations in past and present forest environments, *Adv. Ecol. Res.*, *19*, 111–188.
Gallant, A. J. E., and J. Gergis (2011), An experimental streamflow reconstruction for the River Murray, Australia, 1783–1988, *Water Resour. Res.*, *47*, W00G04, doi:10.1029/2010/WR009832.
Gao, C., A. Robock, and C. Ammann (2008), Volcanic forcing over the past 1500 years: An improved ice core-based index for climate models, *J. Geophys. Res.*, *113*, D23111, doi:10.1029/2008JD010239.
Gergis, J., and L. Ashcroft (2013), Rainfall variations in south-eastern Australia part 2: A comparison of documentary, early instrumental and palaeoclimate records, 1788 – 2008, *Int. J. Climatol.*, *33*, 2973–2987.
Gergis, J., A. Gallant, K. Braganza, D. J. Karoly, K. Allen, L. Cullen, R. D. D'Arrigo, I. Goodwin, P. Grierson, and S. McGregor (2011), On the long-term context of the 1997–2009 'Big Dry' in south-eastern Australia: Insights from a 206-year multi-proxy rainfall reconstruction, *Clim. Change*, *111*, 923–944.
Gou, X., F. Chen, E. Cook, G. Jacoby, M. Yang, and J. Li (2007), Streamflow variations of the Yellow River over the past 593 years in western China reconstructed from tree rings, *Water Resour. Res.*, *43*, W06434, doi:10.1029/2006WR005705.
Grose, M. R., J. Bhend, D. Argueso, M. Ekström, A. J. Dowdy, P. Hoffman, J. P. Evans, and B. Timbal (2015), Comparison of various climate change projections of eastern Australian rainfall, *Aust. Meteorol. Oceanogr. J.*, *65*, 72–89.
Haoglin, D. C., and R. E. Welsch (1978), The hat matrix in regression and ANOVA, *Am. Stat.*, *32*, 17–22.
Hendon, H. H., D. W. Thompson, and M. C. Wheeler (2007), Australian rainfall and surface temperature variations associated with the Southern Hemisphere Annular Mode, *J. Clim.*, *20*, 2452–2467.
Henley, B. J. H, J. Gergis, D. J. Karoly, S. Power, J. Kennedy, and C. K. Folland (2015), A tripole index for the Interdecadal Pacific Oscillation, *Clim. Dyn.*, *45*, 3077–3090.
Ho, M., A. S. Kiem, and D. C. Verdon-Kidd (2015), A palaeoclimate rainfall reconstruction in the Murray-Darling Basin (MDB) Australia: 1. Evaluation of different palaeoclimate archives, rainfall networks and reconstruction techniques, *Water Resour. Res.*, *51*, 8362–8379, doi: 10.1002/2015WR017058.
Holz, G. K., et al. (2010), Climate Futures for Tasmania: Impacts on Agriculture, technical report, Antarct. Clim. and Ecosyst. Coop. Res. Cent., Hobart, Tasmania.
Hope, P., M. R. Grose, B. Timbal, A. J. Dowdy, J. Bhend, J. J. Katzfey, T. Bedin, L. Wilson, and P. H. Whetton (2015), Seasonal and regional signature of projected southern Australian rainfall reduction, *Aust. Meteorol. Oceanogr. J.*, *65*, 54–71.
Isdale, P. J., B. J. Stewart, K. S. Tickle, and J. M. Lough (1998), Palaeohydrological variation in a tropical river catchment: A reconstruction using fluorescent bands in corals of the Great Barrier Reef, Australia, *Holocene*, *8*, 1–8.
Jiayu, H. (1992), Was there a colder summer in China in 1816?, in *The Year Without a Summer*, edited by C. R. Harrington, pp. 448–452, 555pp., Can. Mus. of Nat., Ottawa
Jones, D., W. Wang, and R. Fawcet (2009a), High-quality spatial climate data sets for Australia, *Aust. Meteorol. Oceanogr. J.*, *58*, 233–248.
Jones, J. M., R. L. Fogt, M. Widmann, G. J. Marshall, P. D. Jones, and M. Visbeck (2009b), Historical SAM variability: Part I: Century-length seasonal reconstructions, *J. Clim.*, *22*, 5319–5345.
Kiem, A. S., et al. (2016), Natural hazards in Australia: Droughts, *Clim. Change*, *139*, 37–54.
Lara, A., R. Villalba, and R. Urrutia (2008), A 400-year tree-ring record of the Puelo River summer-fall streamflow in the Valdivian Rainforest eco-region, Chile, *Clim. Change*, *86*, 331–356.
Larsen, S. H., and N. Nichols (2009), Southern Australian rainfall and the subtropical ridge: Variations, interrelationships, and trends, *Geophys. Res. Lett.*, *36*, L08708, doi:10.1029/2009GL037786-.

Lough, J. M. (2011), Great Barrier Reef coral luminescence reveals rainfall variability over northeastern Australia since the 17th century, *Palaeoceanography*, *26*, PA 2201, doi:10.1029/2010PA002050.
McBride, J. L., and N. Nicholls (1983), Seasonal relationships between Australian rainfall and the Southern Oscillation, *Mon. Weather Rev.*, *111*, 1998– 2004.
McGowan, H. A., S. K. Marx, J. Denholm, J. Soderholm, and B. S. Kamber (2009), Reconstructing annual inflows to the headwater catchments of the Murray River, Australia, using the Pacific Decadal Oscillation, *Geophys. Res. Lett.*, *36*, L06707, doi:10.1029/2008GL037049.
Melvin, T. M., and K. R. Briffa (2008), A "signal-free" approach to dendroclimatic standardisation, *Dendrochronologia*, *26*, 71–86.
Melvin, T. M., K. R. Briffa, K. Nicolussi, and M. Grabner (2007), Time-varying-response smoothing, *Dendrochronologia*, *25*, 65–69.
Meyers, G., P. Macintosh, L. Pigot, and M. Pook (2007), The years of El Niño, La Niña, and interactions with the topical Indian Ocean, *J. Clim.*, *20*, 2872–2880.
Mundo, I. A., M. H. Masiokas, R. Villalba, M. S. Morales, R. Neukom, C. Le Quesne, R. B. Urrutia, and A. Lara (2012), Multi-century tree-ring based reconstructions of the Neuquèn River streamflow, northern Patagonia, Argentina, *Clim. Past*, *8*, 815–829.
Murphy, B. F., and B. Timbal (2008) A review of recent climate variability and climate change in southeastern Australia, *Int. J. Climatol.*, *28*, 859–879.
Nichols, N. (2010), Local and remote causes of the southern Australian autumn-winter decline, 1958 – 2007, *Clim. Dyn.*, *34*, 835–845.
Oppenheimer, C. (2003), Climatic, environmental and human consequences of the largest known historic eruption: Tambora volcano (Indonesia) 1815, *Prog. Phys. Geogr.*, *27*, 230–259.
Palmer, J. G., and J. Ogden (1992), Tree-ring chronologies from endemic Australian and New Zealand conifers, in *The Year Without a Summer*, edited by C. R. Harrington, pp. 510–515, Can. Mus. of Nat., Ottawa.
Palmer, J. G., E. R. Cook, C. S. M. Turney, K. J. Allen, P. Fenwick, B. Cook, A. O'Donnell, J. M. Lough, P. J. Baker, and P. Grierson (2015), Drought variability in the eastern Australian and New Zealand summer drought atlas (ANZDA, CE1500–2012) modulated by the Interdecadal Pacific Oscillation, *Environ. Res. Lett.*, *10*, doi:10.1088/1748-9326/10/12/124002.
Parent, C., N. Capelli, A. Berger, M. Crèvecoeur, and J. F. Dat (2008), An overview of plant responses to soil waterlogging, *Plant Stress*, *2*, 20–27.
Pederson, N., C. Leland, B. Nachin, A. E. Hessl, A. E. Bell, D. Martin-Benito, T. Saladyga, B. Suran, P. M. Brown, and N. K. Davi (2013), Three centuries of shifting hydrological regimes across the Mongolian breadbasket, *Agric. For. Meteorol.*, *178-179*, 10–20.
Pezza, A. B., H. A. Rashid, and I. Simmonds (2012), Climate links and recent extremes in antarctic sea ice, high-latitude cyclones, Southern Annular Mode and ENSO, *Clim. Dyn.*, *38*, 57–73.
Pook, M. J., P. C. McIntosh, and G. A. Myers (2006), The synoptic decomposition of cool-season rainfall in the southeastern Australian cropping region, *J. Appl. Meteorol. Climatol.*, *45*, 1156–1170.
Pook, M. J., J. S. Risbey, P. C. McIntosh, C. C. Ummenhofer, A. G. Marshall, and G. A. Meyers (2013), The seasonal cycle of blocking and associated physical mechanisms in the Australian region and relationship with rainfall, *Mon. Weather Rev.*, *141*, 4534–4553.
Power, S., T. Casey, C. Folland, A. Colman, and A. Mehta (1999b), Inter-decadal modulation of the impact of ENSO on Australia, *Clim. Dyn.*, *15*, 319–324.
Power, S. B., and J. Callaghan (2016) Variability in severe coastal flooding in south-eastern Australia since the mid-19th century, associated with storms and death tolls, *J. Appl. Meteorol. Climatol.*, *55*, 1139–1149.
Read, J., and J. R. Busby (1990), Comparative responses to temperature of the major canopy species of Tasmanian cool temperature rainforest and their ecological significance. II Net photosynthesis and climate analysis, *Aust. J. Bot.*, *38*, 185–205.
Risbey, J., M. J. Pook, P. C. McIntosh, M. C. Wheeler, and H. H. Hendon (2009), Remote drivers of Australian rainfall, *Mon Weather Rev.*, *137*, 3233–3253.
Risbey, J., M. Pook, and P. McIntosh (2013), Spatial trends in synoptic rainfall in southern Australia, *Geophys. Res. Lett.*, *40*, 3781–3785, doi: 10.1002/grl.50739.
Ruark, G. A., D. L. Mader, and T. A. Tattar (1983), The influence of soil moisture and temperature on the root growth and vigour of trees: A literature review. Part II, *Aboric. J.*, *7*, 39–51.
Schmidt, G. A., et al. (2011), Climate forcing reconstructions for use in PMIP simulations of the last millennium, *Geosci. Model Dev.*, *4*, 33–45.
Stahle, D. W., J. Villanueva Diaz, D. J. Burnette, J. Ceran Paredes, R. R. Heim Jr., F. K. Fye, R. A. Soto, M. D. Therrell, M. K. Cleaveland, and D. K. Stahle (2011), Major Mesoamerican droughts of the past millennium, *Geophys. Res. Lett.*, *38*, L05703, doi:10.1029/2010GL046472.
Timbal, B., and W. Drosdowsky (2013), The relationship between the decline of southeastern Australian rainfall and the strengthening of the subtropical ridge, *Int. J. Climatol.*, *33*, 1021–1034.
Tozer, C., T. R. Vance, J. L. Roberts, A. S. Kiem, M. A. J. Curran, and A. D. Moy (2016), An ice core derived 1013-year catchment-scale annual rainfall reconstruction in subtropical eastern Australia, *Hydrol. Earth Syst. Sci.*, *20*, 1703–1717.
Trigo, R. M., J. M. Vaqueo, M.-J. Alcoforado, M. Barriendos, J. Taboda, R. Garcia-Herrera, and J. Luterbacher (2009), Iberia in 1816, the year without a summer, *Int. J. Climatol.*, *29*, 99–115.
Trouet, V., and G. J. van Oldenborgh (2013), KMNI Climate Explorer: A web-based research tool for high-resolution palaeoclimatology, *Tree Ring Res.*, *69*, 3–13.
Vance, T. R., J. L. Roberts, C. T. Plummer, A. S. Kiem, and T. D. van Ommen (2014), Interdecadal Pacific variability and eastern Australian megadroughts over the last millennium, *Geophys. Res. Lett.*, *42*, 129–137, doi:10.1002/2014GL062447.
Verdon, D. C., A. M. Wyatt, A. S. Kiem, and S. W. Franks (2004), Multidecadal variability of rainfall and streamflow: Eastern Australia, *Water Resour. Res.*, *40*, W10210, doi:10.1029/2004WR003234.
Verdon-Kidd, D. C., and A. S. Kiem (2009), Nature and causes of protracted droughts in southeastern Australia: Comparison between the Federation, WWII, and Big Dry droughts, *Geophys. Res. Lett.*, *36*, L22707, doi:10.1029/2009GL041067.
Villalba, R., and J. Boninsegna (1992), Changes in southern South American tree-ring chronologies following major eruptions between 1750 and 1970, pp. 493 - 509, in *The year Without a Summer*, edited by C. R. Harrington, 555 pp., Can. Mus. of Nat., Ottawa.
Vinod, H. D., and J. Lòpez-de-Lacalle (2009), Maximum entropy bootstrap for time series: The meboot R package, *J. Stat. Software*, *29*, 1–19.
Visbeck, M. (2009), A station-based Southern Annular Mode Index from 1884 to 2005, *J. Clim.*, *22*, 940–950.
Wigley T. M. L., K. R. Briffa, and P. D. Jones (1984), On the average value of correlated time series with applications in dendroclimatology and hydrometeorology, *J. Clim. Appl. Meteorol.*, *23*, 201–213.
Wilson, C. (1992), Workshop on world climate in 1816: A summary and discussion of results, in *The Year Without a Summer*, C. R. Harrington, pp. 523–556, Can. Mus. of Nat., Ottawa.
Woodhouse, C. A., S. T. Gray, and D. M. Meko (2006), Updated streamflow reconstructions for the Upper Colorado River Basin, *Water Resour. Res.*, *42*, WR05415, doi:10.1029/2005WR004455.